Normative models reveal distinct cortical abnormalities to dimensions of psychopathologies in preadolescents

Qingkun Deng[1], Elizabeth Levitis[2,3], Rick Adams[2,4], Andre Altmann[1]

[1] *UCL Hawkes Institute, Department of Medical Physics and Biomedical Engineering, University College London, London, WC1V 6LJ, UK*

[2] *UCL Hawkes Institute, Department of Computer Science, University College London, London, WC1V 6LJ, UK*

[3] *Section on Developmental Neurogenomics, National Institute of Mental Health, Bethesda, MD, USA*

[4] *Max Planck Centre for Computational Psychiatry and Ageing Research, University College London, London, WC1B 5EH, UK*

Corresponding author:

Qingkun Deng, MRes

University College London

rmapqde@ucl.ac.uk

Short title: distinct cortical abnormalities to psychopathological dimensions

Keywords: adolescent psychopathology, transdiagnostic psychiatry, normative modelling, auto-encoder, latent class analysis, cerebral cortex

Abstract

Background: Evidence suggests a non-specific mapping between psychiatric disorders and underlying neurobiological substrates. A dimensional psychopathology framework may prove useful for organizing observed neurobiological alterations along broad psychopathological dimensions.

Methods: We applied latent class analysis to identify clinical cohorts of symptomatic homogeneity to represent the clinical end of specific psychopathological dimensions (i.e., internalizing/externalizing, *p-factor*), using baseline data ($N = 11860$) from the Adolescent Brain and Cognitive Development (ABCD) Study. These cohorts were compared against neurotypical individuals in terms of deviations from the normality of cortical development, quantified using autoencoder-based normative models, to reveal cortical abnormalities.

Results: We identified cortical thickness as an important MRI-derived index of psychopathology and revealed distinct structural abnormalities to broad psychopathological dimensions.

Conclusion: This study highlights the value of person-centered analytic techniques, combined with normative modeling, to complement traditional associational methodologies in revealing neurobiological correlates of dimensional psychopathologies.

Introduction

To date, most psychiatric neuroimaging studies have been conducted within a case-control study framework, using psychiatric diagnoses to define clinical groups and assuming that neurobiological alterations are uniformly shared within disorders and are distinct between them. This assumption, however, has been disputed by large-scale meta-analyses which have found few diagnostically specific brain morphological changes (1). Instead, common structural changes, such as grey matter reductions in the dorsal anterior cingulate and insula (1), implicated in functional alterations within and between major neurocognitive networks, are found to be shared across psychiatric disorders (2,3). Cumulative evidence, therefore, suggests a non-specific mapping between diagnostic categories and underlying neurobiological abnormalities.

Such a non-specific mapping may be expected given the high rates of psychiatric co-morbidity (e.g., about 40% of adolescents impacted by mental illness have multiple diagnoses (4)), which suggests unitary psychopathological conditions being divided into arbitrary categories (5). Indeed, a large number of symptom-level factor analytic studies have empirically identified transdiagnostic psychopathological dimensions that explain the systematic co-occurrence of symptoms across diagnostic categories (6–8). Evidence from these studies led to the development of dimensional nosology to psychopathology, such as the Hierarchical Taxonomy of Psychopathology (HiTOP) framework (5), conceptualizing psychopathological conditions as continuums with normal to clinical variations, instead of categorical entities.

Two psychopathological dimensions — internalizing and externalizing — received substantial evidence in both adults and adolescents (9). The internalizing dimension reflects an individual's distress expressed inwardly, involving syndromes typically seen in mood disorders such as major depressive disorder and generalized anxiety disorder. The externalizing dimension, on the other hand, reflects overt behavior rendering an individual in social conflict with others, incorporating syndromes seen in, for instance, oppositional defiant disorder and conduct disorder. The two dimensions are moderately and positively correlated with each other (8), which can be accounted for by a higher-order factor of general psychopathology (i.e., *p-factor*) (10), representing a shared susceptibility for developing any mental disorders (11).

A dimensional nosology, as an alternative to the traditional taxonomy, may prove useful for unifying observed neurobiological alterations, non-specifically associated with different disorders, along broad psychopathological dimensions (8). Methodologically, the dimensional modeling quantifies psychopathologies as continuous variables (e.g., factor scores derived from factor analysis), thereby allowing an association analysis (e.g., correlative, regression-based) of the relationships between brain-derived features and psychopathologies. However, while some studies adopting a dimensional approach reported dissociable neurobiological correlates to specific psychopathological dimensions (e.g., fear, internalizing, externalizing) (12–16), others found very few neurobiological correlates unique to distinct psychopathological dimensions and revealed widespread, non-specific, alterations in brain structures associated with higher *p-factor* scores (17–20).

The methodological emphasis on continuous associations has led much of the prior research to identify linear, often univariate, brain-behavior relationships, capturing broad variations across both clinical and non-clinical ranges in behavioral variables. While a simple linear assumption facilitates a straightforward interpretation, such methods disregard the potentially non-linear, non-monotonic, associations that may underlie brain-behavior relationships and relationships between brain-derived features. For instance, if neurobehavioral relations manifest differently between normative and clinically relevant ranges of behavior, neurobiological correlates identified in the previous association studies, involving large non-clinical populations, could be non-characteristic of psychopathologies and therefore non-specific to broad psychopathological dimensions.

Here, we evaluate whether person-centered analytic techniques which identify latent clusters of individuals with phenotypical similarities, may provide a valuable alternative to the study of dimensional psychopathologies and their neurobiological correlates. Specifically, we apply Latent Class Analysis (LCA), with an additional constraint on classification uncertainty, to isolate cohorts of homogeneous, clinically significant behavior syndromes in a large cohort of preadolescents from the Adolescent Brain and Cognitive Development (ABCD) Study. We hypothesize that these psychopathological cohorts, with high symptomatic homogeneity and clinical relevance, may serve precise targets to represent the clinical end of psychopathological dimensions for which specific neurobiological abnormalities can be ascribed.

We focus on the structures of the cerebral cortex and study their abnormalities via *normative modeling (21)*. A normative model maps the individual variations of cortical structures in normative, neurotypical individuals with no behavioral syndromes. Cortical abnormalities of individuals with psychopathologies are, therefore, understood in relation to these variations, quantified as deviations from an expected pattern of normative neurodevelopment. Instead of conventional normative modeling methods (e.g., Gaussian process regression), which establish normality for individual brain features in isolation, we apply autoencoder-based normative models (22) to account for the potentially non-linear spatial interactions between cortical regions, together with squared, non-directional measurement of deviations, without assuming a uni-directional, monotonic manifestation of cortical abnormalities in individuals with similar psychopathologies. We derive cortical abnormalities to specific psychopathological dimensions via group comparisons between clinical cohorts against neurotypical individuals in terms of their quantified deviations from normality. Our approach may provide higher sensitivity for identifying neurobiological abnormalities, compared to linear association analysis and traditional case-control analysis, for its assumption-free modeling of the data and group comparisons in deviations instead of feature values themselves.

Materials and method

Study sample

The ABCD study is a longitudinal study consisting of a demographically diverse sample of over 11,000 children, aged 9-10 at baseline assessment, probabilistically sampled from schools around 21 research sites across the United States (US), involving over 20% of the entire US population in this age range (https://abcdstudy.org/). The recruitment process was detailed in Garavan et al. (23). Ethical review and protocol approval were secured from the Institutional Review Board (IRB) at the University of California, San Diego, and from local IRB approval (24). Parents or guardians gave written informed consent after receiving a full explanation of the procedures, and children provided assent before participating in the study. We used the baseline data from the ABCD Study's Data Release 5.1 ($N = 11868$). We considered all subjects with complete information for the Child Behavior Check List (CBCL) measures (25) ($N = 11860$) (sample characteristics provided in Table S3) for performing LCA, described below. For neuroimaging analysis, we excluded intersex-male subjects ($n = 3$), subjects whose scans failed to pass quality control by the recommended T1-weighted imaging data inclusion criteria or considered by neuroradiologists for clinical referral ($n = 916$), subjects with incomplete information for CBCL measures ($n = 6$) and psychiatric diagnoses (instruments described below, $n = 113$). A final neuroimaging analysis sample of $N = 9021$ unrelated subjects (randomly selecting one subject from each family) were available for normative modelling analysis, described below.

MRI image acquisition and processing

Full details of the MRI acquisition protocols and processing procedures can be found elsewhere (26,27). Briefly, MRI data were collected using 3T scanners, specifically the Siemens Prisma, GE MR 750, and Philips Achieva and Ingenia models, across 21 research sites with harmonized scanning protocols to ensure data consistency. T1-weighted (T1w) images were acquired using a 3D sequence with 1mm isotropic resolution, corrected for gradient nonlinearity distortions using scanner-specific nonlinear transformations. Cortical reconstruction and volumetric segmentation were performed using FreeSurfer v7.1.1 (28). The current study considered cortical features (i.e., cortical thickness, cortical volume, cortical surface area), with cortical regions labelled according to the Destrieux atlas-based classification (mapped to 74 cortical regions per hemisphere; a total of 148 regions) (29).

Behavioral measures

The parent-report CBCL 6-18 were used to measure the behavioral syndrome of adolescents aged 9-10 (25). The CBCL has 113 items divided into syndrome scales including Withdrawn/Depressed, Somatic Complaints, Anxious/Depressed, Rule-Breaking Behavior, Social Problems, Thought Problems, Attention Problems, and Aggressive Behavior. All syndrome scales have a T-score mean of 50 with a standard deviation of 10, with norms adjusted for gender and age groups. Scores on each syndrome scale were dichotomized as either ‘clinically significant’ ($T - score \geq 65$) or ‘normal’ ($T - score < 65$) for performing LCA, described below.

Psychiatric diagnoses

The computerized parent version of the Kiddie Schedule for Affective Disorders and Schizophrenia (KSADS), based on DSM-5 criteria, was used to establish psychiatric diagnoses. We considered lifetime diagnoses for depression, bipolar disorder, anxiety, disruptive mood dysregulation disorder, psychosis, obsessive-compulsive disorder, post-traumatic stress disorder, and attention deficit hyperactivity disorder (ADHD). Following the protocol detailed in Duffy et al. (30), we categorized individuals into larger diagnostic classes based on specific diagnoses within each class. An Autism Spectrum Disorder (ASD) diagnosis was assigned if a parent reported a previous diagnosis.

Latent class analysis

LCA was used to identify latent, or unobserved, subgroups within samples with homogeneities in patterns of responses to observed variables (31). We performed LCA based on the eight CBCL syndrome scales using the R package poLCA (32). We iteratively fitted LCA models from two classes to six classes and selected the final model based on the Bayesian Information Criterion (BIC) (33), which is considered a more reliable fit statistic than others (31,34). The selected LCA model was used to assign each individual to the class with the highest posterior probability. The model's uncertainty in assigning a class membership was measured with

Shannon's entropy (E) (35). We set a constraint on classification uncertainty, only considering samples assigned to latent classes with relatively high certainty ($E \leq 0.2$), to obtain psychopathological cohorts of high symptomatic homogeneity.

Normative modelling

Conditional Variational Autoencoder (cVAE) (36) was used to develop normative models. The cVAE, a variant of the variational autoencoder, aims to learn a probabilistic mapping from the input space X to a latent space Z, from which point estimates can be decoded back to the input space X with minimal reconstruction error (22). The cVAE allows the encoding of the latent space and the decoding for reconstruction to be conditioned on confounding covariates, which helps avoid the need to regress out covariate effect from inputs, which is typically achieved using linear models and may remove unknown sources of variances (37). We had our models conditioned on biological sex (i.e., male/female). Technically, cVAEs are trained to maximize the following evidence lower bound (ELBO) of the marginal log-likelihood of the observed data x, conditioned on the conditional variable c:

$$E_{q_\phi(z|x,c)}[\log p_\theta(x \mid z,c)] - D_{KL}\left(q_\phi(z \mid x,c)||p(z)\right)$$

where the approximate posterior distribution $\mathrm{q}_\phi(z \mid x,c)$ and the conditional likelihood distribution $\mathrm{p}_\theta(x \mid z,c)$ are modelled by the encoder and decoder with parameters ϕ and θ, respectively. The first term, therefore, forces the model to

reduce reconstruction errors, while the second term forces the encoded latent distribution $q(z \mid x, c)$ to be close to the prior distribution $p(z)$, which is chosen as a Gaussian distribution suitable for normative modeling. A cVAE was trained for each of the cortical modalities (i.e., cortical thickness, volume, and surface area), resulting in a total of three normative models. Further technical details on variational autoencoder, model configuration and training details (including data pre-processing), are provided in the Supplement and demonstrated in Figure 1.

Normative cohort

We identified a normative cohort from our neuroimaging analysis sample as subjects without any current or past psychiatric diagnoses (including other psychiatric diagnoses not specified above) and without clinically significant behavioral syndromes ($T - score \geq 65$) for any of the CBCL scales, resulting in a total of $N = 3238$ subjects. The cohort was divided into Training, Validation, and Healthy Controls (HCs) (i.e., Testing set) subsamples randomly sampled from data partitions stratified by sex and household income, using an 8:1:1 split ratio. Distributions of demographic variables for each subset are shown in Figure S1.

Deviation metrics

The metric to quantify the deviation of the whole cortex from normality was derived as the mean square error between the reconstructed feature values and the input feature values (38), as in the below equation:

$$\text{whole cortex deviation} = \frac{1}{\text{number of regions}} \sum_{i=1}^{\text{number of regions}} (x_i - \hat{x}_i)^2$$

where x_i denotes the input value of the i-th cortical region and $\hat{x}_i$ denotes the autoencoder reconstructed value of the i-th cortical region. The assumption behind the metric is that since the cVAE was trained to only encode healthy structures of the cortex, higher reconstruction errors (i.e., deviations) will be observed from processing cortical features of individuals with psychopathologies, whose cortical structures are hypothesized to alter pathologically (38).

The whole cortex deviation metric averages the deviations observed at individual cortical regions. A region-level deviation metric, therefore, allows an investigation of which individual regions tend to exhibit more abnormalities:

$$\text{cortical region deviation} = (x_i - \hat{x}_i)^2$$

where a region level deviation is measured at the i-th cortical region.

To account for reconstruction errors due to an imperfect model fit, we used Cliff's delta (δ_{Cliff}) (a non-parametric effect size metric (39)) to index the degree of abnormality for each region by comparing distribution differences in deviations between psychopathological cohorts and a cohort of neurotypical individuals (i.e.,

HCs, described above). Unlike traditional case-control studies, we note that our method measures effect size based on *deviations* quantified from normative models, instead of feature values themselves. We further assessed the robustness of effect sizes by bootstrapping the training set 1,000 times, creating simulated sets of the same size, and training multiple normative models from these sets to derive bootstrapped confidence intervals (CIs) of effect size for each cortical feature. We consider a cortical feature to exhibit statistically significant abnormality if the lower bound of the 100% CI exceeds 0. Additionally, we only report here the significant features with meaningful effect sizes, indicated by at least a small to medium mean bootstrapped effect size ($\text{mean } \delta_{\text{Cliff}} \geq 0.15$) (40).

Sensitivity analyses

An alternative normative modelling analysis was performed comparing deviations distributions of original latent classes defined by LCA (without applying a constraint on classification uncertainty) against HCs. The results are reported in the Supplement.

Results

Latent class analysis: psychopathological cohorts

Fit statistics for all latent class solutions and a detailed descriptive analysis of the selected solution, including its individual-level classification uncertainty, comparisons between and after an exclusion of high-entropy subjects, are provided in the

Supplement (Table S4-5, Figures S2-6). We selected the four-class solution according to the lowest BIC scores. By applying a constraint on classification uncertainty, we identified three psychopathological cohorts characterized by homogeneous and differential patterns of behavioral syndrome, conceptually close to broad psychopathological dimensions.

Specifically, a cohort with a characteristic elevation of the internalizing syndromes (i.e., Anxious/Depressed, Withdrawn/Depressed, and Somatic), and a relatively high prevalence of thought problems, was identified and thus labeled the *Predominantly Internalizing* cohort. Additionally, a cohort exhibited a characteristic elevation of the externalizing syndromes (i.e., Rule-Break and Aggressive) with a relatively high prevalence of attention problems and was thus labeled the *Predominantly Externalizing* cohort. Lastly, a cohort characterized by high elevations of all syndromes was labeled the *Highly Dysregulated* cohort.

Since some subjects within the psychopathological cohort were not present in the neuroimaging analysis sample due to the exclusion criteria set in the *Sample* Section, they were removed from the normative modeling analysis. Table 1 summarizes the sample characteristics of the remaining sample for each psychopathological cohort against the HCs (demographic information of the original samples in each cohort is provided in Table S5). Figure 2 presents the proportions of remaining samples with clinically significant syndromes, and psychiatric diagnoses, in the cohorts.

Normative modelling: whole cortex deviation

Figure 3A presents the distributions of the whole cortex deviation for each psychopathological cohort compared against the HCs. Given the Shapiro-Wilk tests indicated that none of these deviation scores were normally distributed ($p < .05$; see test results in Table S6), Mann-Whitney U tests (two-sided) were performed to determine statistically significant differences between groups. A false discovery rate (FDR) correction was applied for multiple tests within each modality. We observed a significant difference in cortical thickness for the *Predominantly externalizing* cohort (*FDR-corrected*, $p < .05$, $\delta_{\text{Cliff}} = 0.256$) and the *Highly Dysregulated* cohort (*FDR-corrected*, $p < .05$, $\delta_{\text{Cliff}} = 0.222$). All other comparisons did not reach statistical significance, showing no significant difference in deviations at a whole cortex level.

Normative modeling: individual region deviation

CIs of effect sizes (δ_{Cliff}) for each cortical feature and psychopathological cohort are presented in Figure S6. Figure 3B demonstrates the spatial representation of cortical region abnormalities for each cohort in cortical thickness, volume, and surface area, respectively.

Although no significant difference in deviations was observed at a whole cortex level, an analysis of deviations at individual cortical regions revealed regions at which the *Predominantly internalizing* cohort tends to exhibit significantly higher deviations than HC, including the left transverse frontopolar gyri/sulci and left planum polare of the

superior temporal gyrus in cortical thickness, right middle occipital sulcus and lunatus sulcus in cortical volume, and the left angular gyrus and the right planum temporale in cortical surface area.

In alignment with the significant deviation observed at a whole cortex level, the *Predominantly externalizing* cohort exhibited significantly more deviations at multiple regions in cortical thickness, including the left superior frontal gyrus, left superior frontal sulcus, left vertical ramus of the anterior segment of the lateral sulcus, right precuneus, and right postcentral sulcus. A few other regions also show meaningfully more deviations in other modalities, including the left orbital sulci in cortical volume, and the left planum polare of the superior temporal gyrus in cortical surface area.

Similarly, multiple regions exhibited significantly more deviations in cortical thickness for the *Highly Dysregulated* cohort including the left superior occipital gyrus, left middle occipital sulcus and lunatus sulcus, left medial occipito-temporal sulcus and lingual sulcus, and the right angular gyrus. A few regions showed significantly more deviations including the left superior occipital gyrus, and the right middle occipital sulcus and lunatus sulcus in cortical volume, the left middle frontal gyrus and the right transverse temporal sulcus in cortical surface area.

The sensitivity analysis compared the original latent classes defined by the four-class LCA solution (latent class 2-4, see Figure S2), without applying an constraint on classification uncertainty, against HCs. Except one cortical region (left orbital sulci) showed significantly more deviations with a meaningful mean effect size in cortical

volume for the latent class 3 (see bootstrapped CIs of effect sizes in Figure S8), all other cortical features for each of the latent classes had negligible mean effect sizes ($\text{mean } \delta_{\text{Cliff}} < 0.15$).

Discussion

The current study applied LCA to empirically identify psychopathological cohorts of homogeneous syndrome patterns in a large cohort of preadolescents in the ABCD study. By applying an additional constraint on classification uncertainty, we obtained three psychopathological cohorts, labelled *Predominantly internalizing*, *Predominantly externalizing*, and *Highly Dysregulated*, each characterized by differential elevations of behavioral syndromes clustered clearly into the CBCL internalizing syndrome scales, the externalizing syndrome scales, and all syndrome scales, respectively, thereby representing the clinical end of broad psychopathological dimensions (i.e., internalizing/externalizing, *p-factor*). Due to their high within-cohort symptomatic homogeneities, they served precise symptomatic targets to allow higher sensitivity in identifying syndrome-specific neurobiological abnormalities.

By comparing the psychopathological cohorts against a group of neurotypical individuals in deviations from the normative patterns of cortical structures, our study identified cortical thickness as an important MRI-derived index of psychopathologies in preadolescents from the ABCD baseline dataset, particularly regarding the externalizing syndromes. Notably, this finding contradicts previous association

studies using the same dataset (17–19), which reported robust associations between psychopathologies and cortical volume and surface area, but not cortical thickness.

A potential explanation for this contradiction in findings lies in methodological differences. Our normative modeling approach measures deviations from the normative pattern of cortical thickness in a squared, non-directional manner. In other words, our method captures abnormalities indicative of psychopathologies whether they manifest as abnormal cortical thinning or thickening relative to normal developments seen in neurotypical individuals, thereby providing a more flexible, hypothesis-free, view of structural abnormalities associated with psychopathologies. In contrast, previous studies using a dimensional approach to psychopathologies focus on directional associations between neurological correlates and psychopathologies, operationalized as continuous variables (e.g., factor scores from factor analysis) (17,18,19,41,42). These association studies impose a directional assumption that precludes the possibility of abnormalities in cortical thickness manifested in different directions across individuals with phenotypically similar psychopathologies. Previous association studies, therefore, may suggest a lack of linear, or monotonic, association between cortical thickness and psychopathologies, as opposed to *any* relationships.

Furthermore, our group-level comparisons in deviations at individual cortical regions revealed distinct spatial patterns of cortical abnormalities to divergent psychopathologies, as opposed to highly distributed, non-specific, structural alterations suggested in previous association studies on the ABCD baseline data

(18–20). Specifically, we found localized abnormalities regarding cortical thickness in the left frontopolar cortex (FPC) associated with the *Predominantly internalizing* cohort. Abnormality in this region may complement a structural understanding of previous functional observations on internalizing disorders in adult samples, which report, for instance, reduced functional connectivity of the left FPC to the right lateral orbitofrontal cortex, associated with increased depressive symptoms (43). Furthermore, we found the cohort to exhibit asymmetric abnormalities in the superior temporal gyrus (i.e., left planum polare and right planum temporale), a region implicated in positive symptoms (e.g., hallucinations, thought disturbances) seen in schizophrenia, potentially reflecting the thought problems in the cohort.

The *Predominantly externalizing* cohort, in contrast, showed preferential abnormalities in the left superior frontal cortex (SFC), left Orbitofrontal Cortex (OFC), and right Parietal Cortex (PC) (i.e., postcentral sulcus and Precuneus), primarily in terms of cortical thickness. Abnormalities in these regions are highly consistent with previous findings on externalizing behavior/disorders. In particular, a reduction in the left SFC thickness has been robustly implicated in increased impulsivity, which is associated with inattention, commonly observed in ADHD (44), potentially via its functional role in response inhibition and executive attention (45,46). Similarly, OFC abnormalities, via its altered structural white matter connections with the amygdala (47), have been observed in externalizing behavior/disorders (e.g., conduct disorder) (14,48). Notably, we also identified a structural abnormality in the right PC, a region engaged in goal-directed attentional processing (49), which, together with abnormalities in the SFC and OFC, aligns with attentional dysfunction as a hallmark of externalizing syndromes.

The *Highly Dysregulated* cohort, characterized by the dysregulation profile (50), may conceptually represent the clinical end of the *p-factor* continuum (51), implicating the development of a wide range of syndromes/disorders. Similar to previous findings on the neurological implications of higher *p-factor* scores (18–20), we found the cohort to exhibit a heavier burden of structural disruptions than the other cohorts. However, instead of non-specifically distributed structural disruptions, we found a clear preferential localization of structural abnormalities in the occipital cortex. This finding aligns with Romer and colleagues' works on the *p-factor* (41,42,52), which have associated structural and functional alterations in the occipital cortex with higher *p-factor* scores. Our findings may, therefore, complement this association. Moreover, it is notable that the cohort in our study has a very high prevalence of ASD (*95.05%*, see Figure 2B). This may suggest the observed occipital cortex abnormalities as a neurodevelopment basis of autistic traits (53–55), associated with impairments in social interactions, to mediate the development of psychopathologies in other domains (56).

Our findings should be interpreted in the context of a few methodological limitations. First, we used cohorts of preadolescents with clinically significant psychopathologies to conceptually represent the clinical end of broad psychopathological dimensions. Although such an approach may result in neurobiological correlates of clinical relevance, the subclinical range of variations in these dimensional phenotypes are ignored. Second, our identification of clinical cohorts with high symptomatic homogeneities necessitated the exclusion of large proportions of individuals (see

Table S3 and Supplemental information) with clinically significant syndromes that deviate from the patterns our analysis revealed. This exclusion, therefore, limits the generalizability of our findings to other clinical cohorts (e.g., individuals with only attention problems). Third, although our squared, non-directional, measurement of deviation from normality may increase sensitivity for identifying abnormalities, it simultaneously precludes a directional interpretation both at a group and individual level (e.g., abnormal cortical thickening or thinning). Finally, it is important to note that our cross-sectional analysis can only reveal associative brain-behavioral relations, which precludes any causal interpretations.

In summary, the current study identifies psychopathological cohorts of high symptomatic homogeneity to represent the clinical end of broad psychopathological dimensions and revealed distinct patterns of cortical abnormalities between them. This broad finding, along with our identification of cortical thickness as a significant MRI-derived index of psychopathologies, challenges conclusions from previous association studies using ABCD baseline data. Our study underscores the value of a person-centred analytic approach (e.g., LCA) to complement variable-centred analysis (e.g., factor analysis) in the study of dimensional psychopathologies. When combined with normative modelling (e.g., autoencoder-based normative models), this approach allows group-level comparisons in deviations from normality, quantified from large non-clinical populations, as an alternative to an associational methodology, to offer new insights into the neurobiological correlates of psychopathologies.

References

1. Goodkind M, Eickhoff SB, Oathes DJ, Jiang Y, Chang A, Jones-Hagata LB, *et al.* (2015): Identification of a Common Neurobiological Substrate for Mental Illness. *JAMA Psychiatry* 72: 305–315.

2. McTeague LM, Huemer J, Carreon DM, Jiang Y, Eickhoff SB, Etkin A (2017): Identification of Common Neural Circuit Disruptions in Cognitive Control Across Psychiatric Disorders. *Am J Psychiatry* 174: 676–685.

3. Sha Z, Wager TD, Mechelli A, He Y (2019): Common Dysfunction of Large-Scale Neurocognitive Networks Across Psychiatric Disorders. *Biol Psychiatry* 85: 379–388.

4. Merikangas KR, He J, Burstein M, Swanson SA, Avenevoli S, Cui L, *et al.* (2010): Lifetime Prevalence of Mental Disorders in U.S. Adolescents: Results from the National Comorbidity Survey Replication–Adolescent Supplement (NCS-A). *J Am Acad Child Adolesc Psychiatry* 49: 980–989.

5. Kotov R, Krueger RF, Watson D, Achenbach TM, Althoff RR, Bagby RM, *et al.* (2017): The Hierarchical Taxonomy of Psychopathology (HiTOP): A dimensional alternative to traditional nosologies. *J Abnorm Psychol* 126: 454–477.

6. Achenbach TM (1966): The classification of children's psychiatric symptoms: A factor-analytic study. *Psychol Monogr Gen Appl* 80: 1–37.

7. Forbes MK, Tackett JL, Markon KE, Krueger RF (2016): Beyond comorbidity: Toward a dimensional and hierarchical approach to understanding psychopathology across the life span. *Dev Psychopathol* 28: 971–986.

8. Zald DH, Lahey BB (2017): Implications of the Hierarchical Structure of Psychopathology for Psychiatric Neuroimaging. *Biol Psychiatry Cogn Neurosci Neuroimaging* 2: 310–317.

9. Cosgrove VE, Rhee SH, Gelhorn HL, Boeldt D, Corley RC, Ehringer MA, *et al.* (2011): Structure and Etiology of Co-occurring Internalizing and Externalizing Disorders in Adolescents. *J Abnorm Child Psychol* 39: 109–123.

10. Caspi A, Houts RM, Belsky DW, Goldman-Mellor SJ, Harrington H, Israel S, *et al.* (2014): The p Factor: One General Psychopathology Factor in the Structure of Psychiatric Disorders? *Clin Psychol Sci* 2: 119–137.

11. Lahey BB, Krueger RF, Rathouz PJ, Waldman ID, Zald DH (2017): A hierarchical causal taxonomy of psychopathology across the life span. *Psychol Bull* 143: 142–186.

12. Parkes L, Moore TM, Calkins ME, Cook PA, Cieslak M, Roalf DR, *et al.* (2021): Transdiagnostic dimensions of psychopathology explain individuals' unique deviations from normative neurodevelopment in brain structure. *Transl Psychiatry* 11: 1–13.

13. Snyder HR, Hankin BL, Sandman CA, Head K, Davis EP (2017): Distinct Patterns of Reduced Prefrontal and Limbic Gray Matter Volume in Childhood General and Internalizing Psychopathology. *Clin Psychol Sci* 5: 1001–1013.

14. Ameis SH, Ducharme S, Albaugh MD, Hudziak JJ, Botteron KN, Lepage C, *et al.* (2014): Cortical Thickness, Cortico-Amygdalar Networks, and Externalizing Behaviors in Healthy Children. *Biol Psychiatry* 75: 65–72.

15. Kaczkurkin AN, Moore TM, Calkins ME, Ciric R, Detre JA, Elliott MA, *et al.* (2018): Common and dissociable regional cerebral blood flow differences associate with dimensions of psychopathology across categorical diagnoses. *Mol Psychiatry* 23: 1981–1989.

16. Kaczkurkin AN, Park SS, Sotiras A, Moore TM, Calkins ME, Cieslak M, *et al.* (2019): Evidence for Dissociable Linkage of Dimensions of Psychopathology to Brain Structure in Youths. *Am J Psychiatry* 176: 1000–1009.

17. Blok E, Geenjaar EPT, Geenjaar EAW, Calhoun VD, White T (2022): Neurodevelopmental Trajectories in Children With Internalizing, Externalizing and Emotion Dysregulation Symptoms. *Front Psychiatry* 13. https://doi.org/10.3389/fpsyt.2022.846201

18. Mewton L, Lees B, Squeglia LM, Forbes MK, Sunderland M, Krueger R, *et al.* (n.d.): The relationship between brain structure and general psychopathology in preadolescents - Mewton - 2022 - Journal of Child Psychology and Psychiatry - Wiley Online Library. https://doi.org/10.1111/jcpp.13513

19. Patel Y, Parker N, Salum GA, Pausova Z, Paus T (2022): General Psychopathology, Cognition, and the Cerebral Cortex in 10-Year-Old Children: Insights From the Adolescent Brain Cognitive Development Study. *Front Hum Neurosci* 15. https://doi.org/10.3389/fnhum.2021.781554

20. Neumann A, Muetzel RL, Lahey BB, Bakermans-Kranenburg MJ, van IJzendoorn MH, Jaddoe VW, *et al.* (2020): White Matter Microstructure and the General Psychopathology Factor in Children. *J Am Acad Child Adolesc Psychiatry* 59: 1285–1296.

21. Marquand AF, Kia SM, Zabihi M, Wolfers T, Buitelaar JK, Beckmann CF (2019): Conceptualizing mental disorders as deviations from normative functioning [no. 10]. *Mol Psychiatry* 24: 1415–1424.

22. Lawry Aguila A, Chapman J, Janahi M, Altmann A (2022): Conditional VAEs for Confound Removal and Normative Modelling of Neurodegenerative Diseases. In: Wang L, Dou Q, Fletcher PT, Speidel S, Li S, editors. *Medical*

Image Computing and Computer Assisted Intervention – MICCAI 2022. Cham: Springer Nature Switzerland, pp 430–440.

23. Garavan H, Bartsch H, Conway K, Decastro A, Goldstein RZ, Heeringa S, *et al.* (2018): Recruiting the ABCD sample: Design considerations and procedures. *Dev Cogn Neurosci* 32: 16–22.
24. Auchter AM, Hernandez Mejia M, Heyser CJ, Shilling PD, Jernigan TL, Brown SA, *et al.* (2018): A description of the ABCD organizational structure and communication framework. *Dev Cogn Neurosci* 32: 8–15.
25. Achenbach TM (1999): The Child Behavior Checklist and related instruments. *The Use of Psychological Testing for Treatment Planning and Outcomes Assessment, 2nd Ed*. Mahwah, NJ, US: Lawrence Erlbaum Associates Publishers, pp 429–466.
26. Casey BJ, Cannonier T, Conley MI, Cohen AO, Barch DM, Heitzeg MM, *et al.* (2018): The Adolescent Brain Cognitive Development (ABCD) study: Imaging acquisition across 21 sites. *Dev Cogn Neurosci* 32: 43–54.
27. Hagler DJ, Hatton SeanN, Cornejo MD, Makowski C, Fair DA, Dick AS, *et al.* (2019): Image processing and analysis methods for the Adolescent Brain Cognitive Development Study. *NeuroImage* 202: 116091.
28. Dale AM, Fischl B, Sereno MI (1999): Cortical Surface-Based Analysis: I. Segmentation and Surface Reconstruction. *NeuroImage* 9: 179–194.
29. Destrieux C, Fischl B, Dale A, Halgren E (2010): Automatic parcellation of human cortical gyri and sulci using standard anatomical nomenclature. *NeuroImage* 53: 1–15.

30. Duffy KA, Gandhi R, Falke C, Wiglesworth A, Mueller BA, Fiecas MB, *et al.* (2023): Psychiatric Diagnoses and Treatment in Nine- to Ten-Year-Old Participants in the ABCD Study. *JAACAP Open* 1: 36–47.

31. Weller BE, Bowen NK, Faubert SJ (2020): Latent Class Analysis: A Guide to Best Practice. *J Black Psychol* 46: 287–311.

32. Linzer DA, Lewis JB (2011): poLCA: An R Package for Polytomous Variable Latent Class Analysis. *J Stat Softw* 42: 1–29.

33. Neath AA, Cavanaugh JE (n.d.): The Bayesian information criterion: background, derivation, and applications. https://doi.org/10.1002/wics.199

34. Nylund KL, Asparouhov T, Muthén BO (2007): Deciding on the Number of Classes in Latent Class Analysis and Growth Mixture Modeling: A Monte Carlo Simulation Study. *Struct Equ Model Multidiscip J*. https://doi.org/10.1080/10705510701575396

35. Shannon CE (1948): A mathematical theory of communication. *Bell Syst Tech J* 27: 379–423.

36. Sohn K, Lee H, Yan X (2015): Learning Structured Output Representation using Deep Conditional Generative Models. *Advances in Neural Information Processing Systems*, vol. 28 28. Retrieved May 11, 2024, from https://proceedings.neurips.cc/paper_files/paper/2015/hash/8d55a249e6baa5c06772297520da2051-Abstract.html

37. Kia SM, Huijsdens H, Dinga R, Wolfers T, Mennes M, Andreassen OA, *et al.* (2020): Hierarchical Bayesian Regression for Multi-site Normative Modeling of Neuroimaging Data. In: Martel AL, Abolmaesumi P, Stoyanov D, Mateus D, Zuluaga MA, Zhou SK, *et al.*, editors. *Medical Image Computing and*

Computer Assisted Intervention – MICCAI 2020. Cham: Springer International Publishing, pp 699–709.

38. Pinaya WHL, Scarpazza C, Garcia-Dias R, Vieira S, Baecker L, F da Costa P, *et al.* (2021): Using normative modelling to detect disease progression in mild cognitive impairment and Alzheimer's disease in a cross-sectional multi-cohort study. *Sci Rep* 11: 15746.
39. Macbeth G, Razumiejczyk E, Ledesma RD (2011): Cliff's Delta Calculator: A non-parametric effect size program for two groups of observations. *Univ Psychol* 10: 545–555.
40. Meissel K, Yao ES (2024): Using Cliff's Delta as a Non-Parametric Effect Size Measure: An Accessible Web App and R Tutorial [no. 1]. *Pract Assess Res Eval* 29. https://doi.org/10.7275/pare.1977
41. Elliott ML, Romer A, Knodt AR, Hariri AR (2018): A Connectome-wide Functional Signature of Transdiagnostic Risk for Mental Illness. *Biol Psychiatry* 84: 452–459.
42. Romer AL, Knodt AR, Houts R, Brigidi BD, Moffitt TE, Caspi A, Hariri AR (2018): Structural alterations within cerebellar circuitry are associated with general liability for common mental disorders. *Mol Psychiatry* 23: 1084–1090.
43. Abnormal Functional Connectivity of Frontopolar Subregions in Treatment-Nonresponsive Major Depressive Disorder (2018): *Biol Psychiatry Cogn Neurosci Neuroimaging* 3: 337–347.
44. Schilling C, Kühn S, Paus T, Romanowski A, Banaschewski T, Barbot A, *et al.* (2013): Cortical thickness of superior frontal cortex predicts impulsiveness and perceptual reasoning in adolescence. *Mol Psychiatry* 18: 624–630.

45. Fan J, McCandliss BD, Fossella J, Flombaum JI, Posner MI (2005): The activation of attentional networks. *NeuroImage* 26: 471–479.

46. Sheehan AE, Bounoua N, Miglin R, Spielberg JM, Sadeh N (2021): A multilevel examination of lifetime aggression: integrating cortical thickness, personality pathology and trauma exposure. *Soc Cogn Affect Neurosci* 16: 716–725.

47. Sarkar S, Craig MC, Catani M, Dell'Acqua F, Fahy T, Deeley Q, Murphy DGM (2013): Frontotemporal white-matter microstructural abnormalities in adolescents with conduct disorder: a diffusion tensor imaging study. *Psychol Med* 43: 401–411.

48. Tanzer M, Derome M, Morosan L, Salaminios G, Debbané M (2021): Cortical thickness of the insula and prefrontal cortex relates to externalizing behavior: Cross-sectional and prospective findings. *Dev Psychopathol* 33: 1437–1447.

49. Behrmann M, Geng JJ, Shomstein S (2004): Parietal cortex and attention. *Curr Opin Neurobiol* 14: 212–217.

50. Jordan P, Rescorla LA, Althoff RR, Achenbach TM (2016): International Comparisons of the Youth Self-Report Dysregulation Profile: Latent Class Analyses in 34 Societies. *J Am Acad Child Adolesc Psychiatry* 55: 1046–1053.

51. Deutz MHF, Geeraerts SB, Belsky J, Deković M, van Baar AL, Prinzie P, Patalay P (2020): General Psychopathology and Dysregulation Profile in a Longitudinal Community Sample: Stability, Antecedents and Outcomes. *Child Psychiatry Hum Dev* 51: 114–126.

52. Romer AL, Knodt AR, Sison ML, Ireland D, Houts R, Ramrakha S, *et al.* (2021): Replicability of structural brain alterations associated with general

psychopathology: evidence from a population-representative birth cohort. *Mol Psychiatry* 26: 3839–3846.

53. Jung M, Tu Y, Lang CA, Ortiz A, Park J, Jorgenson K, *et al.* (2019): Decreased structural connectivity and resting-state brain activity in the lateral occipital cortex is associated with social communication deficits in boys with autism spectrum disorder. *NeuroImage* 190: 205–212.

54. Keown CL, Shih P, Nair A, Peterson N, Mulvey ME, Müller R-A (2013): Local Functional Overconnectivity in Posterior Brain Regions Is Associated with Symptom Severity in Autism Spectrum Disorders. *Cell Rep* 5: 567–572.

55. Samson F, Mottron L, Soulières I, Zeffiro TA (2012): Enhanced visual functioning in autism: An ALE meta-analysis. *Hum Brain Mapp* 33: 1553–1581.

56. Dell'Osso L, Lorenzi P, Carpita B (2019): Autistic Traits and Illness Trajectories. *Clin Pract Epidemiol Ment Health CP EMH* 15: 94–98.

Table captions

Table 1: Sample characteristics of the psychopathological cohorts and the HCs.

Figure captions

Figure 1*:* **Analysis pipeline.**

The left side of the figure demonstrates the analysis flow of applying latent class analysis to samples with complete data for the CBCL syndrome scales from the ABCD baseline data. By applying a constraint on classification uncertainty, three psychopathological cohorts were identified. The right side of the figure demonstrates the process of developing normative models using a neuroimaging subsample drawn from the ABCD baseline data. A normative cohort was identified from the neuroimaging sample and was split into three independent sets. A 10-fold cross-validation was performed using the training set to tune a set of hyperparameters for model training. Once the optimal hyperparameters were obtained, final models were obtained using the whole training set and the training was early stopped using a separate validation set to avoid overfitting. The samples in the identified psychopathological cohorts that were present in the neuroimaging sample were compared against the testing set (i.e., HCs) to derived cortical abnormalities to specific psychopathologies.

Figure 2: **Radar charts.**

A – A set of three radar charts demonstrating the proportions of subjects within each of the psychopathological cohort having clinically significant syndromes across the CBCL syndrome scales.

B – A set of three radar charts demonstrating the proportions of subjects within each of the psychopathological cohort having psychiatric diagnoses.

Figure 3: **Cortical abnormalities.**

A – Comparisons in whole cortex deviation distributions of the psychopathological cohorts against the HCs in terms of cortical thickness, volume, surface area. Within each modality, Mann-Whitney U tests with Benjamini–Hochberg FDR correction (correcting for three comparisons tests within each modality) assessed statistical significance: * for $\mathrm{FDR\ corrected\ at\ p} < 0.05$, ** for $\mathrm{FDR\ corrected\ at\ p} < 0.01$, *** for $\mathrm{FDR\ corrected\ at\ p} < 0.001$.

B – Region specific cortical abnormalities in terms of cortical thickness, volume, surface area for each of the psychopathological cohort. Only regions exhibiting significantly, and meaningfully, higher deviations $(\mathrm{mean}\ \delta_{\mathrm{Cliff}} \geq 0.15)$ are plotted in red.

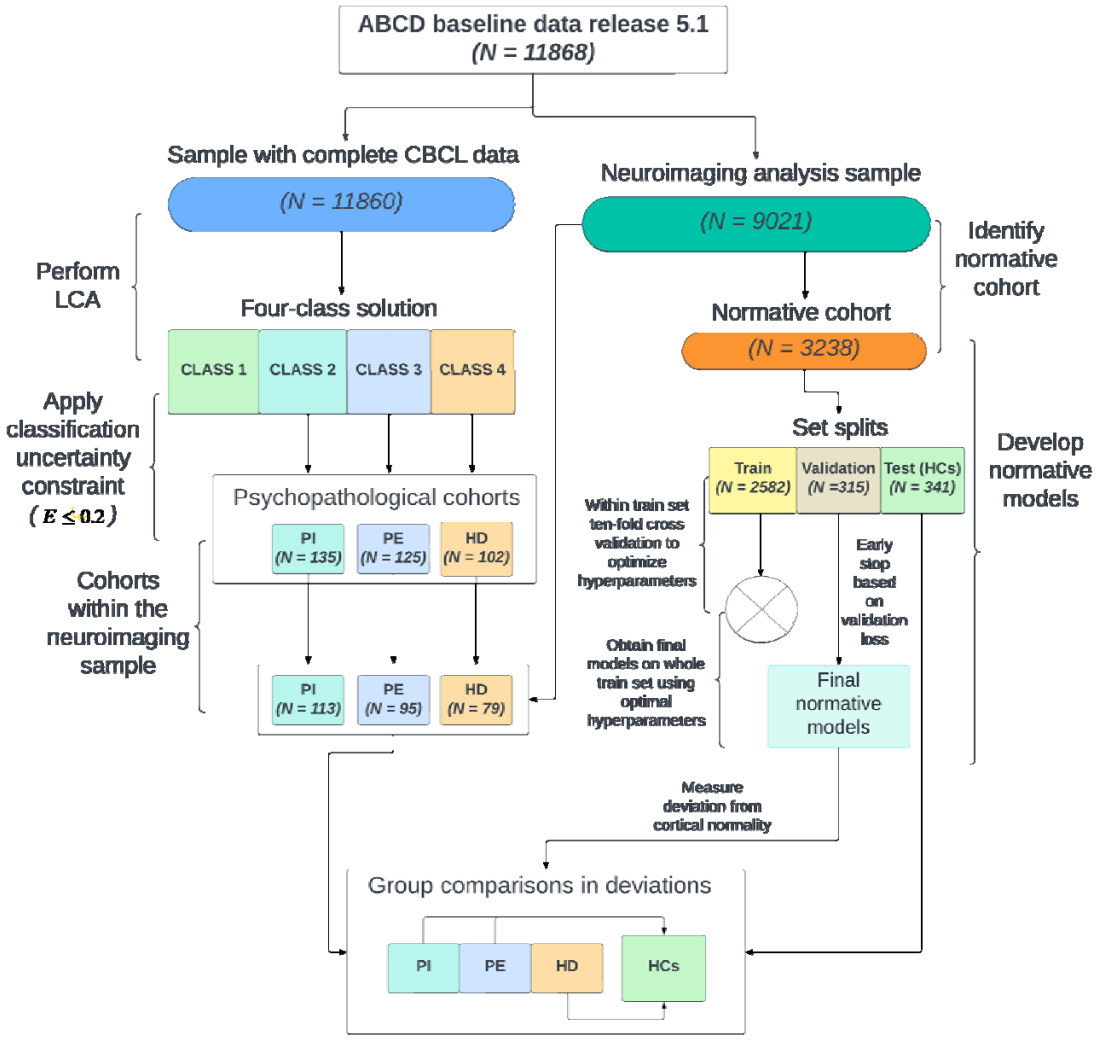
ABCD baseline data release 5.1
(N = 11868)
Sample with complete CBCL data
(N = 11860)
Neuroimaging analysis sample
(N = 9021)
Perform LCA
Identify normative cohort
Four-class solution
CLASS 1
CLASS 2
CLASS 3
CLASS 4
Normative cohort
(N = 3238)
Apply classification uncertainty constraint
(E ≤ 0.2)
Set splits
Train
(N = 2582)
Validation
(N =315)
Test (HCs)
(N = 341)
Develop normative models
Psychopathological cohorts
PI
(N = 135)
PE
(N = 125)
HD
(N = 102)
Within train set ten-fold cross validation to optimize hyperparameters
Early stop based on validation loss
Cohorts within the neuroimaging sample
PI
(N = 113)
PE
(N = 95)
HD
(N = 79)
Obtain final models on whole train set using optimal hyperparameters
Final normative models
Measure deviation from cortical normality
Group comparisons in deviations
PI
PE
HD
HCs

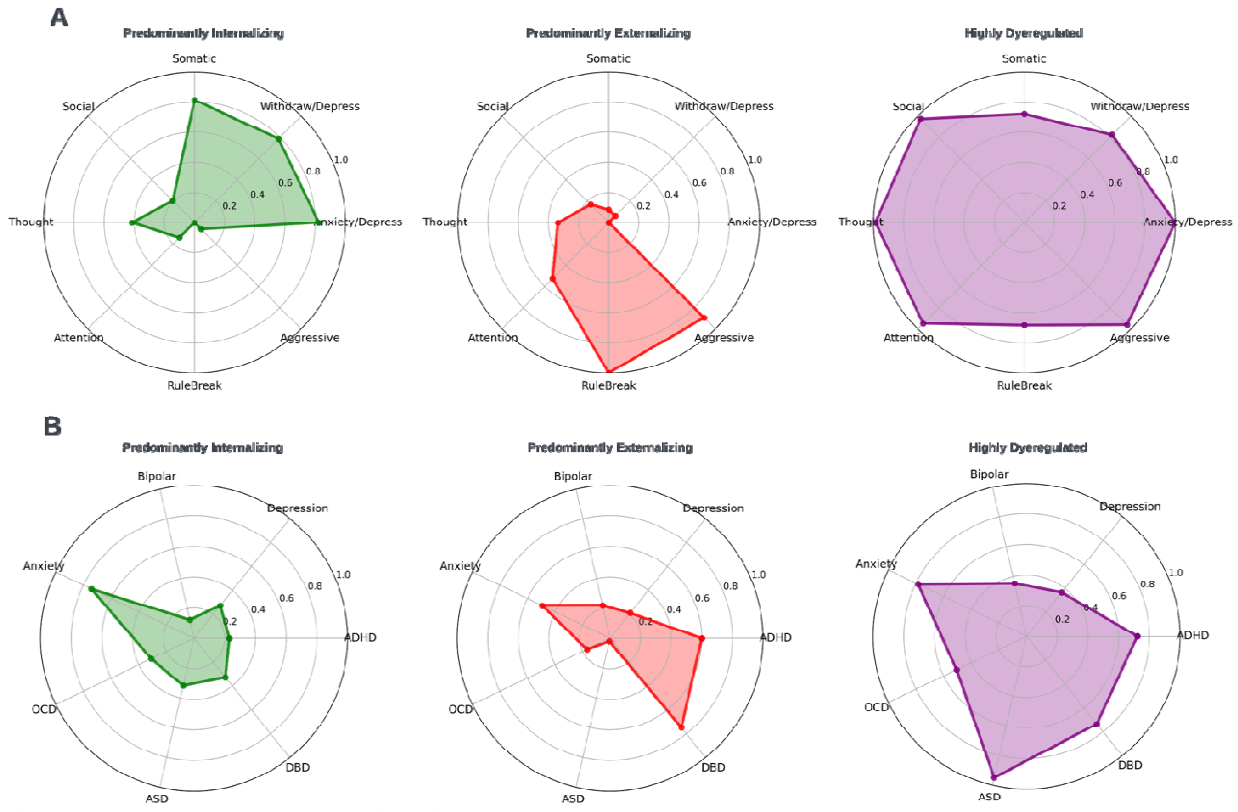
A
Predominantly Internalizing
Predominantly Externalizing
Highly Dyeregulated
Somatic
Withdraw/Depress
Anxiety/Depress
Aggressive
RuleBreak
Attention
Thought
Social
0.2
0.4
0.6
0.8
1.0
B
Bipolar
Depression
ADHD
DBD
ASD
OCD
Anxiety

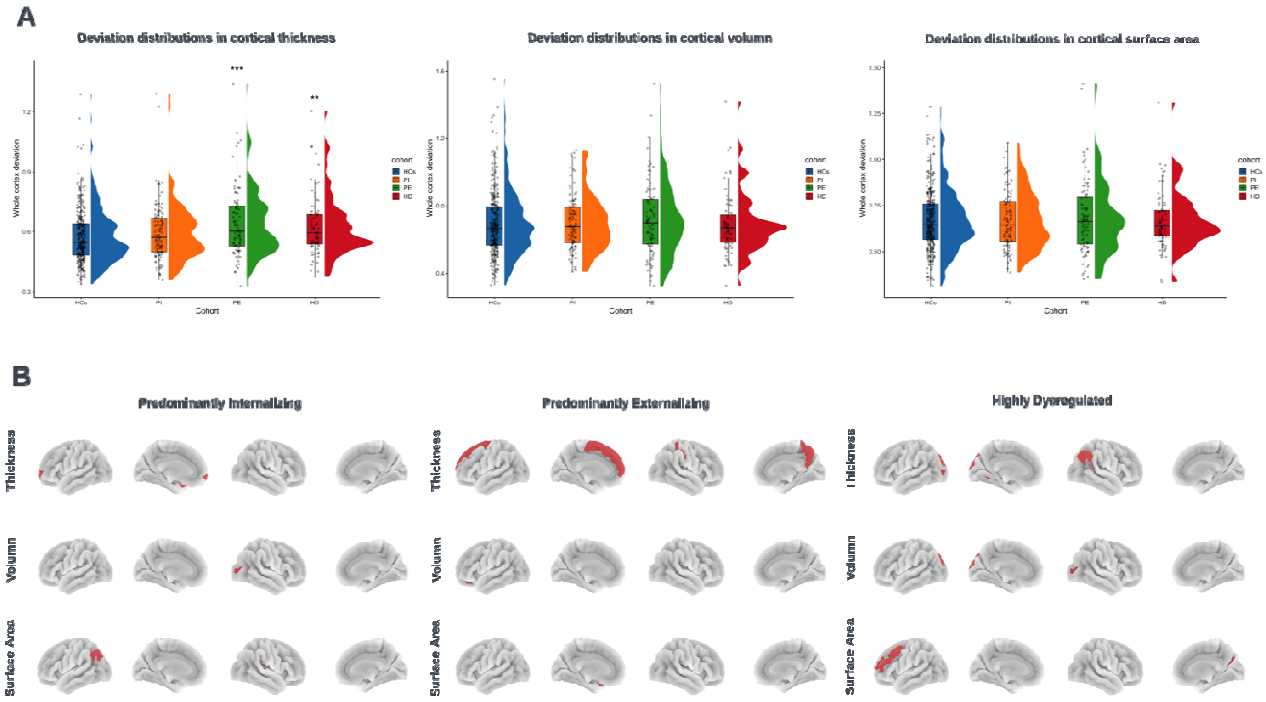
A
Deviation distributions in cortical thickness
Deviation distributions in cortical volumn
Deviation distributions in cortical surface area
Whole cortex deviation
Cohort
HCs
PI
PE
HD
***
**
B
Predominantly Internalizing
Predominantly Externalizing
Highly Dyeregulated
Thickness
Volumn
Surface Area

	Healthy controls	Predominantly internalizing	Predominantly externalizing	Highly dysregulated
N	341	113	95	79
Biological sex, n (%)				
Male	162 (47.5%)	53 (46.9%)	57 (60.0%)	53 (67.1%)
Female	179 (52.5%)	60 (53.1%)	38 (40.0%)	26 (32.9%)
Age in months				
mean (SD)	118.83 (7.22)	119.44 (7.11)	119.16 (7.41)	118.94 (7.17)
Race/ethnicity, n (%)				
White	177 (51.9%)	55 (48.7%)	36 (37.9%)	32 (40.5%)
Black	52 (15.2%)	7 (6.2%)	31 (32.6%)	16 (20.3%)
Hispanic	70 (20.5%)	35 (31.0%)	9 (9.5%)	20 (25.3%)
Asian	12 (3.5%)	1 (0.9%)	0 (0.0%)	0 (0.0%)
Other	30 (8.8%)	15 (13.3%)	19 (20.0%)	11 (13.9%)
Annual income in $, n (%)				
< 5,000	12 (3.5%)	1 (0.9%)	10 (10.5%)	12 (15.2%)
5,000 - 11,999	12 (3.5%)	3 (2.7%)	11 (11.6%)	9 (11.4%)
12,000 - 15,999	9 (2.6%)	7 (6.2%)	4 (4.2%)	3 (3.8%)
16,000 - 24,999	15 (4.4%)	4 (3.5%)	5 (5.3%)	7 (8.9%)
25,000 - 34,999	18 (5.3%)	14 (12.4%)	12 (12.6%)	7 (8.9%)
35,000 - 49,999	26 (7.6%)	18 (15.9%)	6 (6.3%)	7 (8.9%)
50,000 - 74,999	39 (11.4%)	16 (14.2%)	12 (12.6%)	10 (12.7%)
75,000 - 99,999	45 (13.2%)	10 (8.8%)	4 (4.2%)	4 (5.1%)
100,000 - 199,999	94 (27.6%)	26 (23.0%)	19 (20.0%)	7 (8.9%)
> 200,000	40 (11.7%)	7 (6.2%)	3 (3.2%)	3 (3.8%)
Not Provided	31 (9.1%)	7 (6.2%)	9 (9.5%)	10 (12.7%)